Charge-Separation in Uranium Diazomethane Complexes Leading to C−H Activation and Chemical Transformation

Oanh P. Lam,[†,‡] Patrick L. Feng,[†] Frank W. Heinemann,[‡] Joseph M. O'Connor,[†] and Karsten Meyer*,[‡]

University of California, San Diego, Department of Chemistry, 9500 Gilman Drive, La Jolla, California 92093, and University of Erlangen-Nürnberg, Department of Chemistry and Pharmacy, Inorganic Chemistry, Egerlandstr. 1, D-91058 Erlangen, Germany

Received September 4, 2007; E-mail: KMeyer@chemie.uni-erlangen.de

Abstract: The reaction of diphenyldiazomethane with $[((^{t-Bu}ArO)_3tacn)U^{III}]$ (**1**) results in an η^2-bound diphenyldiazomethane uranium complex. This complex exhibits unusual electronic properties as a charge-separated species with a radical anionic open-shell ligand, $[((^{t-Bu}ArO)_3tacn)U^{IV}(\eta^2\text{-NNCPh}_2)]$ (**2**). Treating Ph_2CN_2 with a uranium complex that contains a sterically more demanding adamantane functionalized ligand, $[((^{Ad}ArO)_3tacn)U^{III}]$ (**3**) results in an unprecedented C−H activation and nitrogen insertion to produce a five-membered heterocyclic indazole complex, $[((^{Ad}ArO)_3tacn)U^{IV}(\eta^2\text{-3-phen(Ind)})]$ (**5**). X-ray crystallography and spectroscopic characterization of these two compounds show that the $[((^{t-Bu}ArO)_3tacn)U^{IV}(\eta^2\text{-NNCPh}_2)]$ compound is a U(IV) complex with a radical anionic ligand, whereas $[((^{Ad}ArO)_3tacn)U^{IV}(\eta^2\text{-3-phen(Ind)})]$ is a U(IV) f^2 species with a closed-shell ligand.

Introduction

In recent years, there has been increasing development in the field of uranium coordination and organometallic chemistry.[1−3] The covalency in uranium ligand bonds is weaker than that of the d-block transition metals.[4] Regardless, the participation of f-orbitals has been shown to be important in bonding and has been documented for oxidation states ranging from +III to +VI.[5−9] Trivalent uranium's ability to make use of its f orbitals in bonding, coupled with the propensity to participate in one- and two-electron reductions,[7,10−12] has made this actinide ion an attractive candidate for small molecule activation.[9,13,14] Our group has demonstrated that using sterically encumbering

ligands chelated to uranium, we can successfully activate small molecules such as organic azides,[15] CO,[16] and CO$_2$.[17] Inspired by the previously reported O-coordinated η^1-CO$_2$ uranium complex $[((^{Ad}ArO)_3tacn)U^{IV}(CO_2^{•-})]$,[17] which revealed unusual electronic properties as a charge-separated species with a radical anionic ligand, we were interested in further studying the possibilities for unique chemical transformations related to this type of complexes. In principle, a one-electron reduction of diazoalkanes could produce such a charge-separated complex with a radical anionic ligand.

Diazoalkanes have received much attention in the past three decades as reactive substrates for organometallic complexes. They have been used as models for dinitrogen activation, since the diazoalkane N≡N bond often mimics N$_2$ binding to metal centers.[18] Diphenyldiazomethane also has been used frequently as a carbene source via N$_2$ loss for the synthesis of transition metal carbene complexes, such as the Ni(II) diphenylcarbene complex (Figure 1, top).[19−21]

However, investigations into the reactivity of these molecules with actinide complexes have been surprisingly scarce. To date, such studies have been limited to the research done by Burns

---

† University of California, San Diego.
‡ University of Erlangen-Nürnberg.
(1) Evans, W. J.; Kozimor, S. A.; Ziller, J. W. *Science* **2005**, *309*, 1835−1838.
(2) Hayton, T. W.; Boncella, J. M.; Scott, B. L.; Palmer, P. D.; Batista, E. R.; Hay, P. J. *Science* **2005**, *310*, 1941−1943.
(3) Summerscales, O. T.; Cloke, F. G. N.; Hitchcock, P. B.; Green, J. C.; Hazari, N. *Science* **2006**, *311*, 829−831.
(4) Marks, T. J. *Progress in Inorganic Chemistry*; John Wiley & Sons: New York, 1979; Vol. 25.
(5) Streitwieser, A.; Müller-Westerhoff, U. *J. Am. Chem. Soc.* **1968**, *90*, 7364.
(6) Avdeef, A.; Raymond, K. N.; Hodgson, K. O.; Zalkin, A. *Inorg. Chem.* **1972**, *11*, 1083−1088.
(7) Diaconescu, P. L.; Arnold, P. L.; Baker, T. A.; Mindiola, D. J.; Cummins, C. C. *J. Am. Chem. Soc.* **2000**, *122*, 6108−6109.
(8) Meyer, K.; Mindiola, D. J.; Baker, T. A.; Davis, W. M.; Cummins, C. C. *Angew. Chem., Int. Ed.* **2000**, *39*, 3063−3066.
(9) Brennan, J. G.; Andersen, R. A.; Robbins, J. L. *J. Am. Chem. Soc.* **1986**, *108*, 335−336.
(10) Castro-Rodriguez, I.; Nakai, H.; Meyer, K. *Angew. Chem., Int. Ed.* **2006**, *45*, 2389−2392.
(11) Diaconescu, P. L.; Cummins, C. C. *J. Am. Chem. Soc.* **2002**, *124*, 7660−7661.
(12) Warner, B. P.; Scott, B. L.; Burns, C. J. *Angew. Chem., Int. Ed.* **1998**, *37*, 959−960.
(13) Cloke, F. G. N.; Hitchcock, P. B. *J. Am. Chem. Soc.* **2002**, *124*, 9352−9353.
(14) Roussel, P.; Errington, W.; Kaltsoyannis, N.; Scott, P. *J. Organomet. Chem.* **2001**, *635*, 69−74.

(15) Castro-Rodriguez, I.; Olsen, K.; Gantzel, P.; Meyer, K. *J. Am. Chem. Soc.* **2003**, *125*, 4565−4571.
(16) Castro-Rodriguez, I.; Meyer, K. *J. Am. Chem. Soc.* **2005**, *127*, 11242−11243.
(17) Castro-Rodriguez, I.; Nakai, H.; Zakharov, L. N.; Rheingold, A. L.; Meyer, K. *Science* **2004**, *305*, 1757−1759.
(18) Schramm, K. D.; Ibers, J. A. *Inorg. Chem.* **1980**, *19*, 1231−1236.
(19) Broring, M.; Brandt, C. D.; Stellwag, S. *Chem. Commun.* **2003**, 2344−2345.
(20) Li, Y.; Huang, J.-S.; Zhou, Z.-Y.; Che, C.-M.; You, X.-Z. *J. Am. Chem. Soc.* **2002**, *124*, 13185−13193.
(21) Mindiola, D. J.; Hillhouse, G. L. *J. Am. Chem. Soc.* **2002**, *124*, 9976−9977.

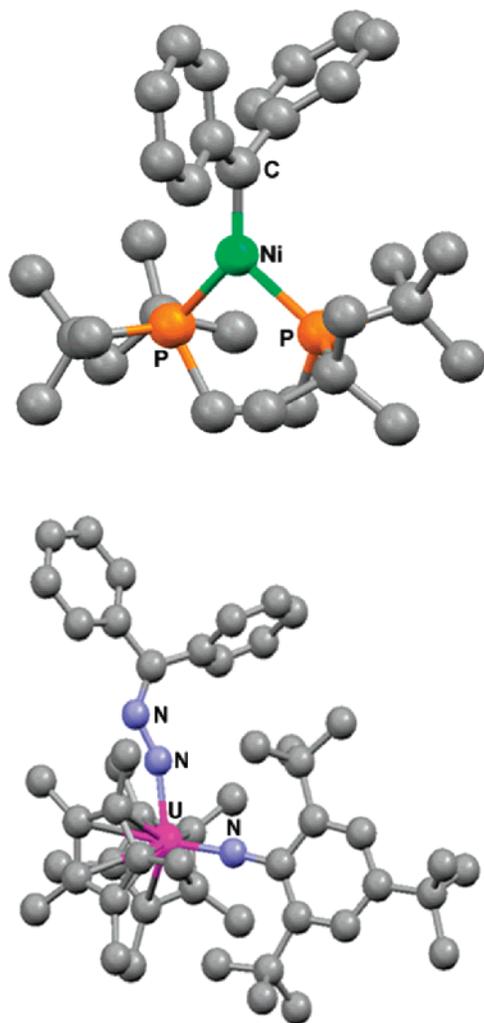**Figure 1.** Molecular structure of Ni(II) diphenylcarbene complex, [(dtbpe)-Ni(CPh₂)][21] (CCDC 193129) (top) and U(VI) bis(imido) complex, [(C₅-Me₅)₂U(N-2,4,6-*t*-Bu₃C₆H₂)(NNCPh₂)][22] (CCDC 172876) (bottom).

and co-workers at the Los Alamos National Laboratory, who have reported the U(VI) bis(imido) complex (Figure 1, bottom).[22,23]

Herein, we report the results from our studies of the reaction of the six-coordinate U(III) precursor complexes [((^{R}ArO)$_3$tacn)-U^{III}] (R = *t*-Bu, Ad) with diphenyldiazomethane. Crystallographic and spectroscopic characterization are presented for a unique actinide η^2-bound diphenyldiazomethane and an indazole complex arising from an unusual transformation promoted by C–H activation and subsequent N-insertion of a reactive intermediate complex with a radical anionic ligand.

Results

Synthesis and Molecular Structure of 2. Treatment of a red-brown solution of [(($^{t-Bu}$ArO)$_3$tacn)U^{III}] (**1**) in pentane with 1 equiv of diphenyldiazomethane at room temperature results in an orange solution within minutes. Orange solids of [(($^{t-Bu}$-ArO)$_3$tacn)U^{IV}(η^2-NNCPh$_2$)] (**2**, Scheme 1) are isolated from a cold pentane solution in good yield. Recrystallization from a concentrated pentane solution at −40 °C gives XRD-quality

crystals of **2**. The molecular structure of **2** in crystals of **2**·2C₅H₁₂ (Figure 2) shows an eight-coordinate complex with diphenyl-diazomethane bound in an η^2 fashion through the two nitrogen atoms. This represents a rather unique phenomenon since eight-coordinate complexes are uncommon in the [((^{R}ArO)$_3$tacn)U] system due to the denticity and steric demand of the hexadentate ligand. Compared to **1**, bonding interactions with the ($^{t-Bu}$ArO)$_3$tacn^{3-} ligand in **2** remain unaltered as seen by the typical average U−O(ArO) and U−N(tacn) bond distances of 2.20 and 2.70 Å, respectively (Table 1). The U1−N4 distance of 2.259(4) Å is comparable to the corresponding U−N distance of 2.25(2) Å in Burns' η^2 hydrazonato complex, [(C₅Me₅)₂U($\eta^2(N,N')$-CH₃−NN=CPh₂)(OTf)].[23] Structural parameters indicate U−N4 is an amide and U−N5 is a dative bond as shown by the much longer U1−N5 bond length of 2.582(4) Å. Most interesting are the N4−N5 and the N5−C52 bond lengths of 1.338(5) Å and 1.333(6) Å, consistent with bond orders between one and two. For comparison, these deviate from free *p*-bromo diphenyldiazomethane N−N and C−N bond lengths of 1.135 and 1.287 Å.[24] Additionally, the angles around C52 sum up to 359.98° clearly identifying that C52 is sp² hybridized.

The metrical parameters found in **2** imply that the single electron is delocalized over the C−N−N unit. Despite the good quality XRD data, there are no structural indications that the single electron in **2** is delocalized into the phenyl rings, as no significant disruptions in C−C bond lengths are observed. Defined as the displacement of the uranium atom below the triangular plane of the three phenolic oxygens, the uranium out-of-plane shift (U_{oop}) is an important structural parameter to monitor in complexes of the [((^{R}ArO)$_3$tacn)U] system because it indicates the strength of metal−ligand interaction.[25] This parameter, which is a function of U−L orbital involvement and electrostatic interaction, increases as the formal oxidation state increases. Hence, as the U center is pulled toward the plane, there is a decrease in the out-of-plane shift. For reference, the uranium out-of-plane shift for the six-coordinate starting complexes **1** and **3** is U_{oop} = −0.75 and −0.88 Å, respectively. The U_{oop} shift of −0.151 Å for complex **2** is very small compared to that of the starting complex **1**. In comparison, this U_{oop} value is consistent with that of the U imido complexes [(($^{t-Bu}$ArO)$_3$tacn)U^V(N(SiMe$_3$))] and [((^{Ad}ArO)$_3$tacn)U^V-(N(SiMe$_3$))] (U_{oop} = −0.151 and −0.188 Å respectively) with U≡N distances reported as 1.985(5) and 2.122(2) Å, respectively.[25] Hence, the strong uranium−imido bond in **2** correlates well with the observed small uranium out-of-plane shift.

Due to minor f-orbital involvement in U−L bonding compared to transition metal bonding, we suggest a highly polarized bond between U1 and the amide N4 bond (Ph₂C=N5=N4). Since normal uranium−amide single bond lengths are slightly longer, the short U1−N4 bond length of 2.259(4) Å and the small out-of-plane shift of −0.151 Å suggest multiple bonding similar to that found in U(V) imido complexes. For instance, the average U−N bond length in [U(N(SiMe₃)₂)₃] is 2.32 Å.[26] From metrical parameters it is proposed that the axial ligand in complex **2** is a radical anionic species resulting from a one-electron reduction of diphenyldiazomethane by the strongly

(22) Kiplinger, J. L.; Morris, D. E.; Scott, B. L.; Burns, C. J. *Chem. Commun.* **2002**, 30−31.
(23) Kiplinger, J. L.; John, K. D.; Morris, D. E.; Scott, B. L.; Burns, C. J. *Organometallics* **2002**, *21*, 4306−4308.
(24) Iikubo, T.; Itoh, T.; Hirai, K.; Takahashi, Y.; Kawano, M.; Ohashi, Y.; Tomioka, H. *Eur. J. Org. Chem.* **2004**, 3004−3010.
(25) Castro-Rodriguez, I.; Meyer, K. *Chem. Commun.* **2006**, 1353−1368.
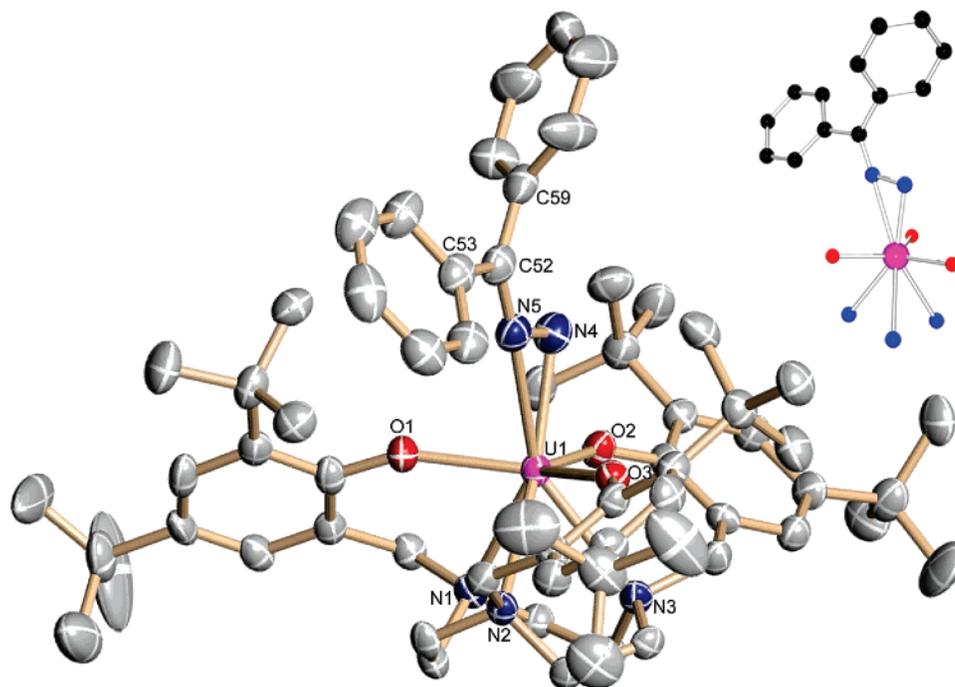(26) Stewart, J. L.; Andersen, R. A. *Polyhedron* **1998**, *17*, 953−958.

Figure 2. Molecular structure of [(($^{t-Bu}$ArO)$_3$tacn)U^{IV}(η^2-NNCPh$_2$)] in crystals of **2**·2C$_5$H$_{12}$. Thermal ellipsoids are at 50% probability level. Hydrogen and cocrystallized solvent molecules are omitted for clarity.

Scheme 1. Scheme of Synthesis of Compounds **2**, **4**, and **5** from Precursor Complexes [((^{R}ArO)$_3$tacn)U^{III}] with R = *t*-Bu (**1**) and Ad (**3**)
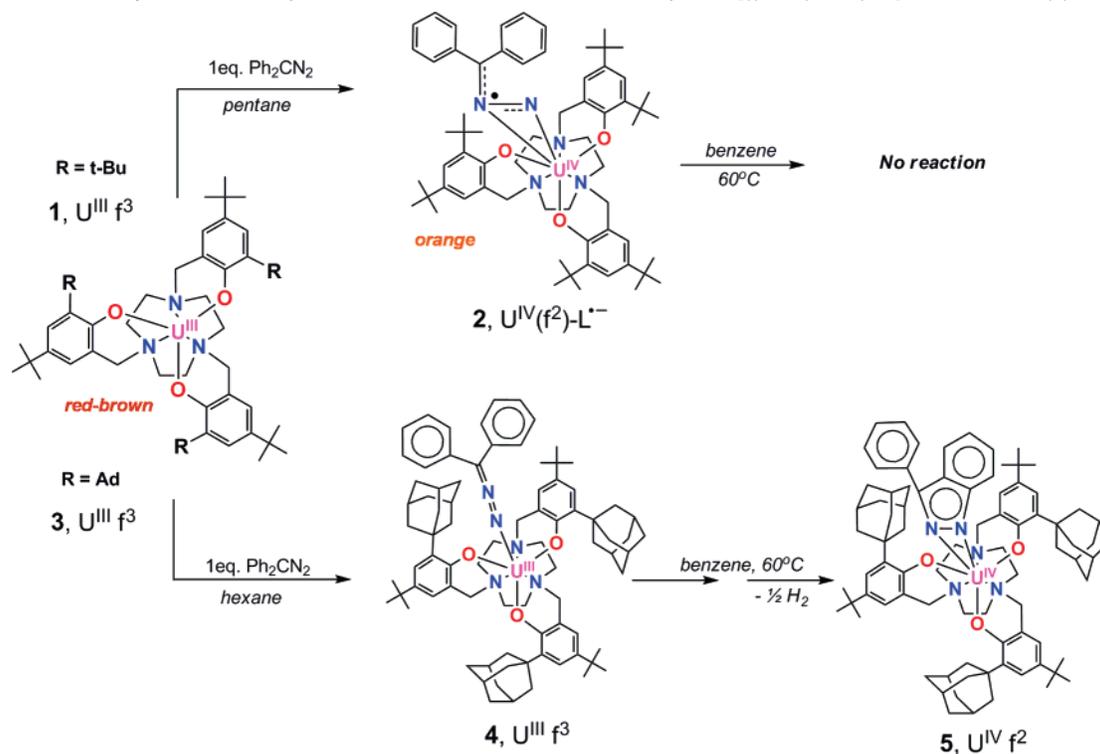
reducing U(III) center. This idea was further probed using magnetic and spectroscopic techniques.

Magnetism and Electronic Absorption of 2. Variable temperature SQUID magnetization and electronic absorption data support the proposed electronic structure of **2** (Figure 3, top) as a charge-separated species with a radical anionic ligand. Typically, for U(IV) f^2 complexes, the variable temperature magnetization trace exhibits a μ_{eff} range of ~0.5 μ_B to ~3 μ_B (4 to 300 K).[25] The low μ_{eff} is due to a nonmagnetic singlet

electronic ground state at low temperature.[27] The magnetization curve of **2** shows a low-temperature magnetic moment of μ_{eff} ~1.75 μ_B, much higher than that expected and observed for other U(IV) f^2 complexes [((^{R}ArO)$_3$tacn)U—L] with axially bound closed-shell ligands L = Cl$^-$, Br$^-$, I$^-$, N$_3$$^-$.[25] The increased μ_{eff} at 4 K is attributed to the magnetic contribution from the unpaired radical electron delocalized over the C—N—N

(27) Stewart, J. L.; Andersen, R. A. *New J. Chem.* **1995**, *19*, 587−595.
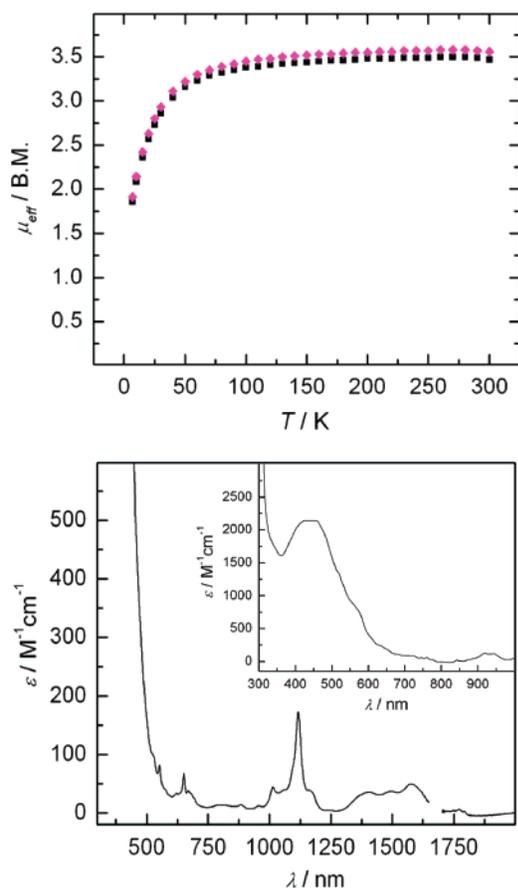
Figure 3. Temperature-dependent SQUID magnetization data (at 1 T) for sample **2** plotted as magnetic moment (μ_{eff}) vs temperature (*T*) (top). Data were corrected for underlying diamagnetism, and reproducibility was checked on two independently synthesized samples. Electronic absorption spectrum for sample **2** (bottom) with an inlay of the absorption spectrum of **1** for comparison, both recorded in benzene.

Table 1. Selected Structural Parameters for Complexes **2**, **5**, and **6** (Bond Distances in Å, Angles in deg)

structural parameters	2	5	6
U–N1$_{tacn}$	2.725(4)	2.780(2)	2.669(3)
U–N2$_{tacn}$	2.675(3)	2.600(2)	2.709(3)
U–N3$_{tacn}$	2.704(3)	2.785(2)	2.722(3)
U–N$_{av}$	2.701	2.722	2.700
U–O1$_{ArO}$	2.200(3)	2.2066(19)	2.186(2)
U–O2$_{ArO}$	2.181(3)	2.1630(17)	2.192(3)
U–O3$_{ArO}$	2.201(3)	2.1789(19)	2.208(3)
U–O$_{av}$	2.194	2.183	2.195
U–N4	2.259(4)	2.419(2)	2.381(12)
U–N5	2.582(4)	2.533(2)	2.598(8)
N4–N5	1.338(5)	1.388(3)	1.348(15)
N5–C52	1.333(6)	1.352(4)	1.249(12)
U–N4–N5	87.8(3)	78.30(14)	83.4(7)
N4–N5–C52	122.8(4)	110.7(2)	117.7(10)
N5–C52–C59	120.7(4)	108.0(3)	109.1(9)
Σ∠ C52	359.98		
$U_{out-of-plane\ shift}$	−0.151	−0.265	−0.150
3–5 dihedral		19.23(12)	2.75(59)
5–6 dihedral		0.98(18)	1.82(67)

unit of the η^2 coordinated Ph$_2$CN$_2$ ligand. The same magnetic behavior was observed for the U(IV) complex with the one-electron reduced CO$_2$ ligand in [((^{Ad}ArO)$_3$tacn)U^{IV}(CO$_2$$^{•-}$)].[17]

The UV/vis/NIR spectrum of a pale orange benzene solution of **2** was acquired at room temperature. The absorption spectrum for tetravalent uranium complex **2** (Figure 3, bottom) includes an inlay of the absorption spectrum for the trivalent f^3 precursor complex **1**. It is apparent that the spectrum of f^2 complex **2** lacks the intense and color-giving $5f^3$ to $5f^26d^1$ transition at 441 nm ($\epsilon = 2140$ M^{-1} cm^{-1}), resulting from coordination and reduction of Ph$_2$CN$_2$. For most mid- to high-valent actinides, the 6*d* levels lie well above the 5*f*. Accordingly, the corresponding metal-centered $5f^n$ to $5f^{(n-1)}6d^1$ transitions appear below 200 nm of their electronic absorption spectra. Consequently, complexes of U(IV) only give rise to relatively narrow, line-like spectra in the visible and near-infrared regions. These Laporte-forbidden *f*–*f* transitions differ from the analogous bands in lanthanide spectra in that owing to covalency greater intensities and broader linewidths result.[4] The *f*–*f* transition bands ($\epsilon = 25-175$ M^{-1} cm^{-1}) that spread over the UV–vis and NIR region are very similar to those of the uranium CO$_2$ complex, which has been characterized previously as a charge-separated U(IV) complex with a coordinated radical anion.[17] The IR spectrum exhibits no N=N stretch for free Ph$_2$CN$_2$ ($\nu_{N=N} = 2040$ cm^{-1}).[24] This is consistent with η^2 binding and partial reduction in **2**, where the N=N bond is weakened significantly, with the stretch being obscured into the fingerprint region of the spectrum. Taken together, the spectroscopic data support **2** as a charge-separated U(IV) complex with a radical anionic Ph$_2$CN$_2$ ligand coordinated side-on at the axial position. Multiple attempts at observing EPR signals for complex **2** were made, however, without success. Samples of complex **2**, either in the solid-state or in solution, were found to be EPR silent (perpendicular mode X-Band) at room and cryogenic temperatures (as low as 4 K).[28]

Synthesis and Molecular Structure of 5. Treating the precursor complex [((^{Ad}ArO)$_3$tacn)U^{III}] (**3**), bearing the sterically more encumbering adamantane functionalized ligand, with 1 equiv of diphenyldiazomethane in hexane at room temperature results in an orange-green precipitate (66% yield). The product was collected by vacuum filtration and characterized as the seven-coordinate complex [((^{Ad}ArO)$_3$tacn)U^{III}(η^1-NNCPh$_2$)] (**4**). Spectroscopic characterization suggests that the Ph$_2$CNN ligand is an axial ligand bound to the uranium center in a linear η^1-N fashion. Transformation to a heterocyclic indazole product occurs upon heating complex **4** in benzene at 60 °C for 1 h in high yield. Recrystallization from diffusion of acetonitrile into a solution of tetrahydrofuran yields green crystals. An X-ray diffraction study on a single crystal obtained from slow diffusion of THF into an acetonitrile solution reveals an eight-coordinate complex [((^{Ad}ArO)$_3$tacn)U^{IV}(η^2-3-phen(Ind))] (**5**), where a newly formed 3-phenyl indazole ligand is η^2-N,N bound to the uranium center. The molecular structure of **5** is presented in Figure 4. Average U–O(ArO) and U–N(tacn) distances of 2.18 and 2.72 Å, respectively, are as expected (Table 1). The U1–N4 and U1–N5 bond lengths of 2.419(2) and 2.533(2) Å are in the range typically observed for U–N single bonds. The five- and six-membered rings are close to planar with a small deviation from planarity of merely 0.98°. The bond lengths within the five-membered ring are nearly equivalent, ranging from 1.37 (N4–N5) to 1.43 Å (C71–C72). These can be described as having bond orders of 1.5, supporting the fact that the five- and six-membered ring system is aromatic, possessing a total of 10 π-electrons, and thus satisfying Hückel's Rule. The uranium ion in complex **5** has a U_{oop} shift of −0.265 Å and,

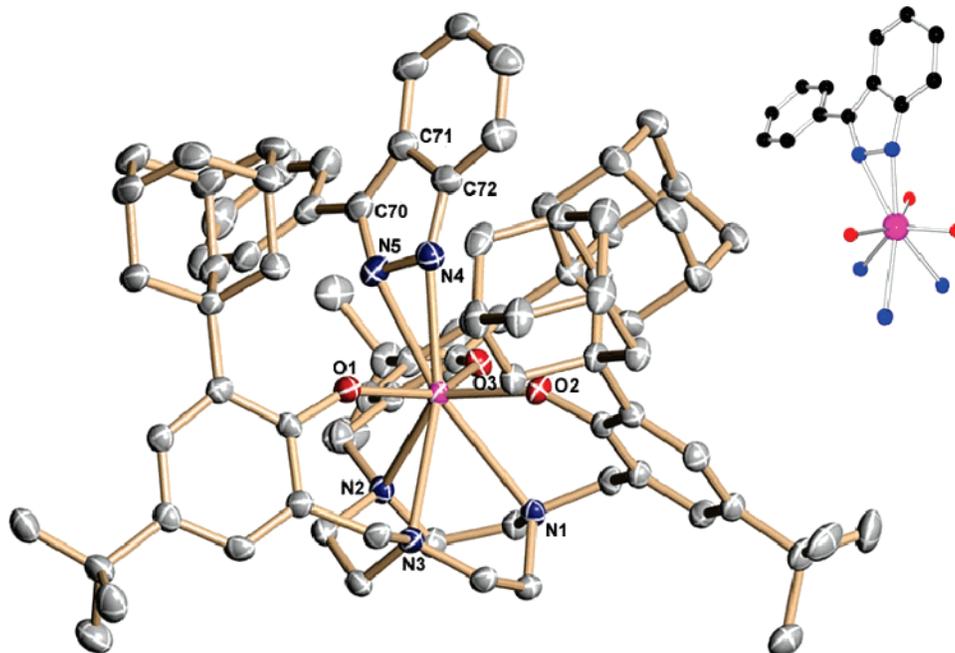(28) Ursu, I.; Lupei, V. *Bull. Magn. Reson.* **1984**, *6*, 162–227.

Figure 4. Molecular structure of $[((^{Ad}ArO)_3tacn)U^{IV}(\eta^2\text{-}3\text{-phen(Ind)})]$ in crystals of **5**. Crystals were grown from diffusion of acetonitrile into THF. Thermal ellipsoids are at 50% probability level. Hydrogen atoms are omitted for clarity. Cocrystallized solvents are absent in the crystal lattice.

accordingly, has a much longer U–N4 bond length of 2.419(2) Å than that found in **2** (d(U–N4) = 2.259(4) Å, U_{oop} = −0.151 Å). This is expected, since the nature of the ligand has changed from a strongly coordinating η^1-imido-type N ligand (as seen in **2**) to an η^2-bound indazole in **5**.

Magnetism and Electronic Absorption for 4 and 5. XRD-quality crystals for **4** could not be obtained, and thus, no structural information is available for the intermediate complex **4**. However, from elemental analysis, SQUID magnetization, electronic absorption, and ^{1}H NMR spectroscopy, the structure of **4** can be deduced. Variable temperature SQUID magnetization data clearly indicate a trivalent U ion in complex **4** (Figure 5, top). A plot of effective magnetic moment vs temperature displays μ_{eff} values ranging from 1.9 to 2.9 μ_B (5–300 K). The temperature-dependency and μ_{eff} values are very similar to those of other trivalent complexes of the $[((^RArO)_3tacn)U]$ system, including those of the precursor complex **3**. Also, the electronic absorption spectra of **3** and **4** are similar. The UV/vis/NIR spectrum of green-orange **4** obtained in benzene solution exhibits an intense $5f^3$ to $5f^26d^1$ metal-centered, Laporte-allowed electronic transition at 418 nm (ϵ = 5410 M^{-1} cm^{-1}) characteristic of a U(III) complex (Figure 5, bottom). In contrast to U(IV) complexes, U(III) transitions are parity-allowed, and thus, high-intensity absorption bands arising from $5f^3$ to $5f^26d^1$ transitions appear in the visible and near-UV region of the spectrum. In SrCl$_2$ single crystals doped with U^{3+}, for instance, the transition from the lowest level of the $^4I_{9/2}$ ground state of the U(III) f^3 configuration to crystal-field levels resulting from the $5f^26d^1$ manifold has been observed as intense bands at energies as low as 600 nm, which shift appreciably depending on the bound ligands.[29,30] The $5f^3$ to $5f^26d^1$ transition for complex **4** has undergone a blue shift compared to the precursor **3**, which exhibits the $5f^3$ to $5f^26d^1$ transition at 441 nm (ϵ = 2140 M^{-1} cm^{-1}). The IR spectrum (KBr) features a nearly

(29) Karbowiak, M. *J. Phys. Chem. A* **2005**, *109*, 3569−3577.
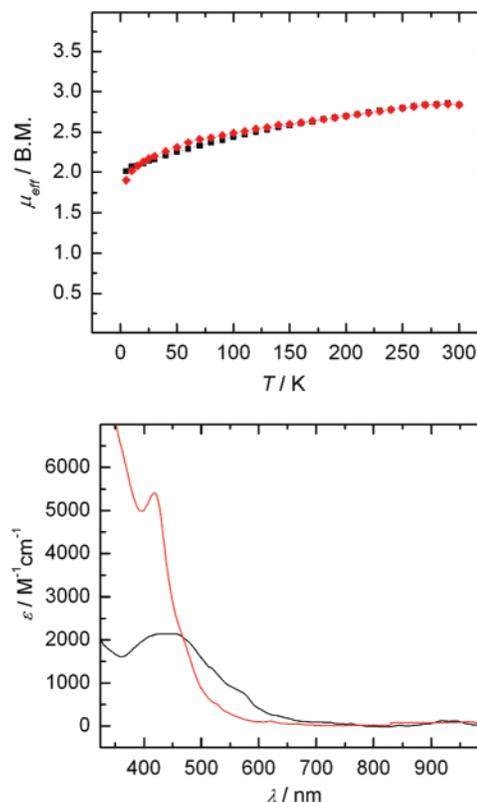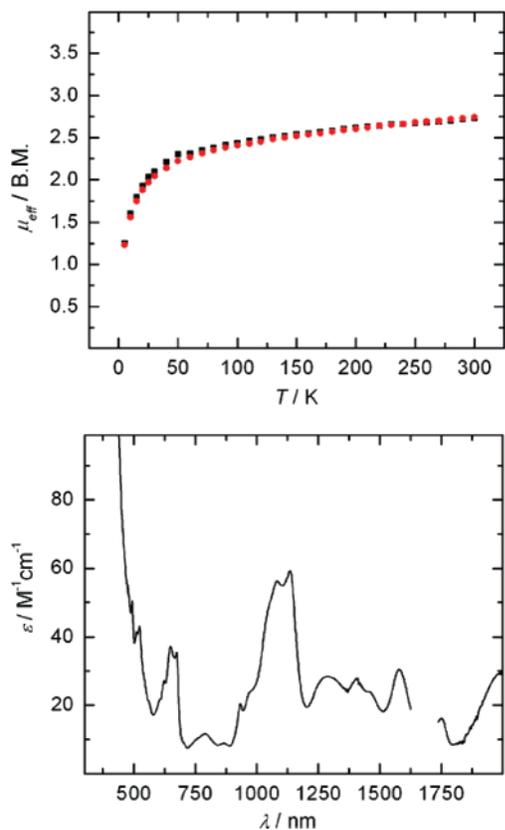(30) Karbowiak, M.; Drożdżyński, J. *J. Phys. Chem. A* **2004**, *108*, 6397−6406.

Figure 5. Temperature-dependent SQUID magnetization data (at 1 T) for sample **4** plotted as magnetic moment (μ_{eff}) vs temperature (T) (top). Data were corrected for underlying diamagnetism, and reproducibility was checked on two independently synthesized samples. For comparison, the electronic absorption plot features both **3** (black) and **4** (red) in C$_6$H$_6$ (bottom).

unperturbed ν(N=N) stretch at 2036 cm^{-1} that is close to that of free diphenyldiazomethane (2040 cm^{-1}); however, it is emphasized that no free diphenyldiazomethane was present as determined by ^{1}H NMR spectroscopy and CHN elemental analysis of the isolated material (see Experimental Section). In

Figure 6. Temperature-dependent SQUID magnetization data (at 1 T) for sample **5** plotted as magnetic moment (μ_{eff}) vs temperature (T) (top). Data were corrected for underlying diamagnetism, and reproducibility was checked on two independently synthesized samples. Electronic absorption spectrum of **5** in CH$_2$Cl$_2$ (bottom).

addition, free rotation of the Ph$_2$CN$_2$ ligand produces an idealized C_3 symmetric molecule, explaining the 19 resonances seen in the ^{1}H NMR spectrum of **4** acquired in benzene-d_6, at room temperature.

From this spectroscopic data and steric considerations, we conclude that intermediate **4** is a U(III) complex with an η^1-N bound diphenyldiazomethane ligand, N=N=CPh$_2$. We suggest a structure similar to those found in [((^{Ad}ArO)$_3$tacn)U—X], where X is a rod-like hetero-cumulene ligand such as O=C=O, N=N=N, or N=C=N—Me linearly coordinated in the cylindrical cavity supported by the three bulky adamantyl substituents.[25] Because the initial coordination of Ph$_2$CN$_2$ does not involve redox chemistry, the N=N stretch remains virtually unperturbed upon binding.

The subsequent transformation of **4** into **5** involves the formation of 0.5 equiv of dihydrogen, which was detected by gas chromatography with a thermal conductivity detector (GC-TCD). The ^{1}H NMR spectrum of transformed species **5**, obtained in benzene-d_6, shows two *tert*-butyl resonances, indicating C_s symmetry. IR spectroscopy of **5** as a KBr pellet revealed the disappearance of the N=N stretch (2036 cm^{-1}) after **4** underwent nitrogen insertion and coordination to the uranium center. Variable temperature SQUID magnetization data of **5** show a temperature-dependent behavior, varying from 1.2 μ_B at 5 K to 2.7 μ_B at 300 K (Figure 6, top). This temperature dependency is characteristic of other U(IV) complexes such as the U(IV) azide complex [((^{Ad}ArO)$_3$tacn)U(N$_3$)] and U^{IV} halide species [((^{Ad}ArO)$_3$tacn)U(X)] (X = Cl, Br, I).[25] The electronic
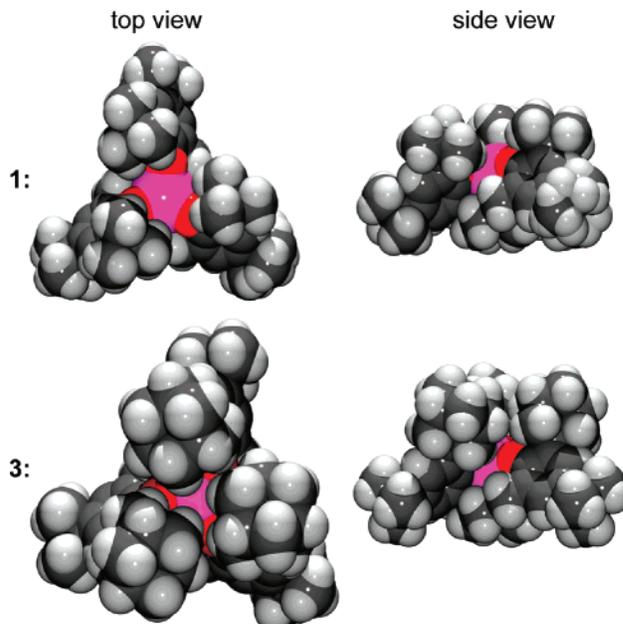

Figure 7. Space-filling representations of **1** (top) and **3** (bottom). Top views (left) and side views (right) are also shown.
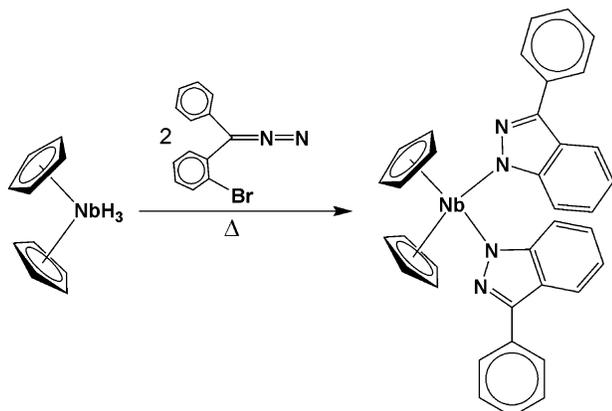
absorption spectrum obtained in benzene of green **5** exhibits sharp transitions between 500 and 2000 nm ($\epsilon = 10-60$ M^{-1} cm^{-1}) (Figure 6, bottom). These are attributed to $f-f$ transitions expected for U(IV) complexes supporting **5** as a U(IV) species possessing a closed-shell ligand.

Discussion

As frequently reported, when diphenyldiazomethane coordinates to metals in an η^2 fashion, it involves insertion of the α-N into a pre-existing M—L bond to form hydrazonato complexes. Such is the case for Zr and Ti, which produce the hydrazonato species [(Cp)$_2$Zr(Me)(η^2-Ph$_2$C=N—NMe)][31] and [(Cp*)Ti(Me)(η^2-Ph$_2$C=N—NMe)][Ti(Cp*)(Me$_2$)](μ-O),[32] as well as for Burns' uranium methyl triflato complex [(Cp*)$_2$U(CH$_3$)-(OTf)][23] (Scheme 2), which all contain M—C bonds necessary for N-insertion. Although [(($^{t\text{-Bu}}$ArO)$_3$tacn)U] (**1**) is comprised solely of the hexadentate aryloxide triazacyclononane ligand (without M—C bonds), η^2 coordination of Ph$_2$CN$_2$ to the U center still occurs, hence forming the unprecedented actinide η^2-N,N bound diphenyldiazomethane (**2**) (Scheme 1). Complex **2** is a charge-separated complex that possesses a radical anionic ligand, Ph$_2$CNN$^{•-}$. Such compounds are appreciated not only for their rarity but also for their interesting spectroscopic character.[33−35]

The separate products obtained from the reaction of diphenyldiazomethane with the two different uranium systems **1** and **3** perfectly illustrate how steric alterations of the ligand can result in significant changes in reactivity. From the space filling model of **1** (Figure 7, top), it is clear that the bowl-shaped

(31) Gambarotta, S.; Floriani, C.; Chiesi-Villa, A.; Guastini, C. *Inorg. Chem.* **1983**, *22*, 2029−2034.
(32) Serrano, R.; Flores, J. C.; Royo, P.; Mena, M. *Organometallics* **1989**, *8*, 1404−1408.
(33) Evans, W. J.; Drummond, D. K. *J. Am. Chem. Soc.* **1989**, *111*, 3329−3335.
(34) Edelstein, N. M.; Allen, P. G.; Bucher, J. J.; Shuh, D. K.; Sofield, C. D. *J. Am. Chem. Soc.* **1996**, *118*, 13115−13116.
(35) Schultz, M.; Boncella, J. M.; Berg, D. J.; Tilley, T. D.; Andersen, R. A. *Organometallics* **2002**, *21*, 460−472.
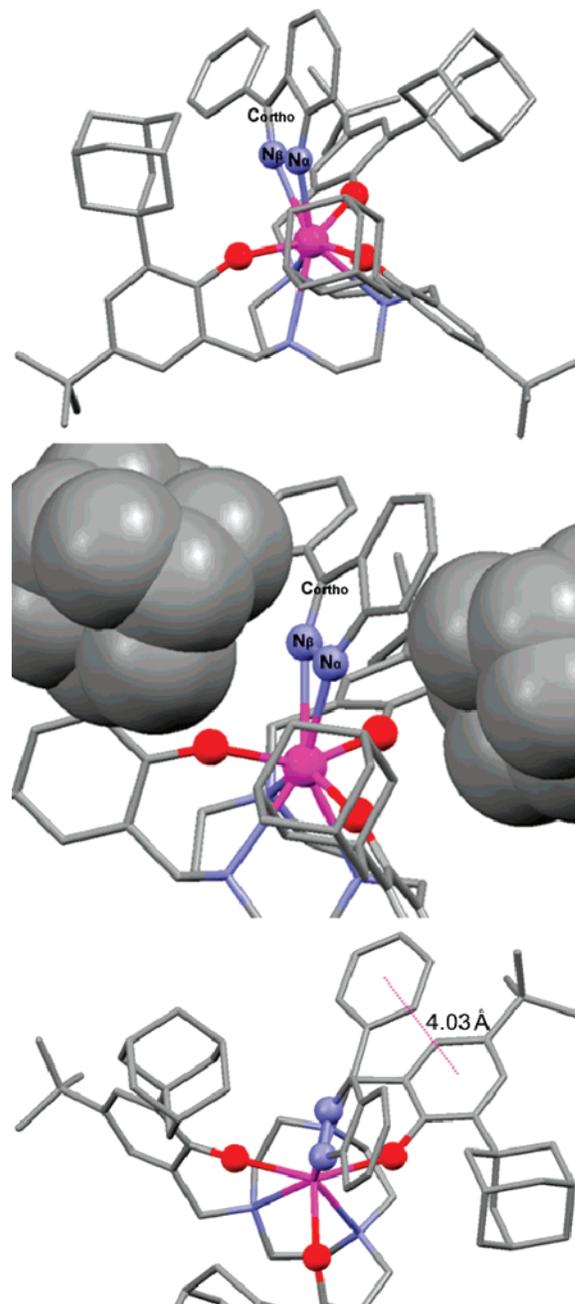
Scheme 2. Diphenyldiazomethane Insertion into the U−CH₃ Bond to Form a Uranium Triflato Hydrazonato Complex (Burns et al.)[23]
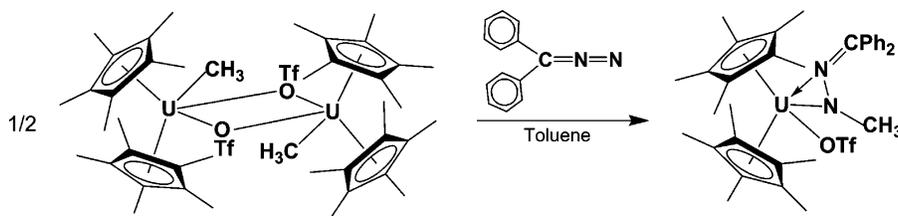
Scheme 3. 3-Phenyl Indazole Formation through C−Br Activation of 2-Bromodiphenyldiazomethane (Lemenovskii et al.)[36]


coordination product was identified as a "nitrene complex," and upon heating this product, cyclometalation was proposed through nitrogen insertion into the C−H bond of a nearby *tert*-butyl group to produce [(C₅Me₅)₂U(=N−2,4,6-ᵗBu₃C₆H₂)(=N−N=

reactive site is much more accessible than the 5 Å-deep cylindrical reactive site of **3** (Figure 7, bottom).

For this reason, the less sterically pressured **2** does not undergo nitrogen insertion when heated because the phenyl groups are allowed to freely rotate making N-insertion into the C−H bond not entropically favorable. The nitrogen insertion leading to **5** is attributed to the steric pressure exerted on the diphenyldiazomethane fragment by the adamantane groups (and possibly a weak π−π interaction), thereby placing a phenyl ring in plane with the N−N−U plane and allowing the electron-rich imido-type α-N (N4) closer to the ortho phenyl C−H bond for insertion (Figure 8). Steric pressure describes the force exerted on a substrate by the sterics of its environment thereby influencing the substrate's spatial orientation, binding mode, and reactivity. Accordingly, our proposition that steric pressure helps trigger the N-insertion is supported by the observation of bending in the indazole unit in **5**, resulting in the dihedral angle of 19.2° between the three- and five-membered rings (see complex **6**).

The transformation of diphenyldiazomethane into 3-phenyl-indazole is rare and, to the best of our knowledge, has only been previously reported by Lemenovskii.[36] In Lemenovskii's work, the reaction of niobocene trihydride with *o*-bromodiphenyldiazomethane produced a bis-indazole species in low yield (Scheme 3). Our high-yield transformation is even more unexpected, given that activating the phenyl C−H bond (∼110 kcal/mol)[37] is more difficult than the corresponding C−Br bond (70.9 kcal/mol).[38] A related transformation was also observed for Burns' U(IV) imido complex [(Cp*)₂U(=N−2,4,6-ᵗBu₃C₆H₂-Ar)]. When reacted with diphenyldiazomethane, the first

(36) Lemenovskii, D. A.; Putala, M.; Nikonov, G. I.; Kazennova, N. B. *J. Organomet. Chem.* **1993**, *454*, 123−131.
(37) McMillen, D. F.; Golden, D. M. *Annu. Rev. Phys. Chem.* **1982**, *33*, 493−532.
(38) Szwarc, M.; Williams, D. *Proc. R. Soc. London, Ser. A* **1953**, *219*, 353−366.

Figure 8. Structural representations of **5** illustrating how steric constraints by bulky adamantane group and π−π interactions place one of the two benzene rings of Ph₂CN₂ in plane with the N−N−U plane for C−H activation and N insertion. The dihedral angle of 19.2° between the three- and five-membered rings is also caused by steric pressure.

Scheme 4. Proposed Synthetic Pathways for Complexes **2**, **4**, and **5**
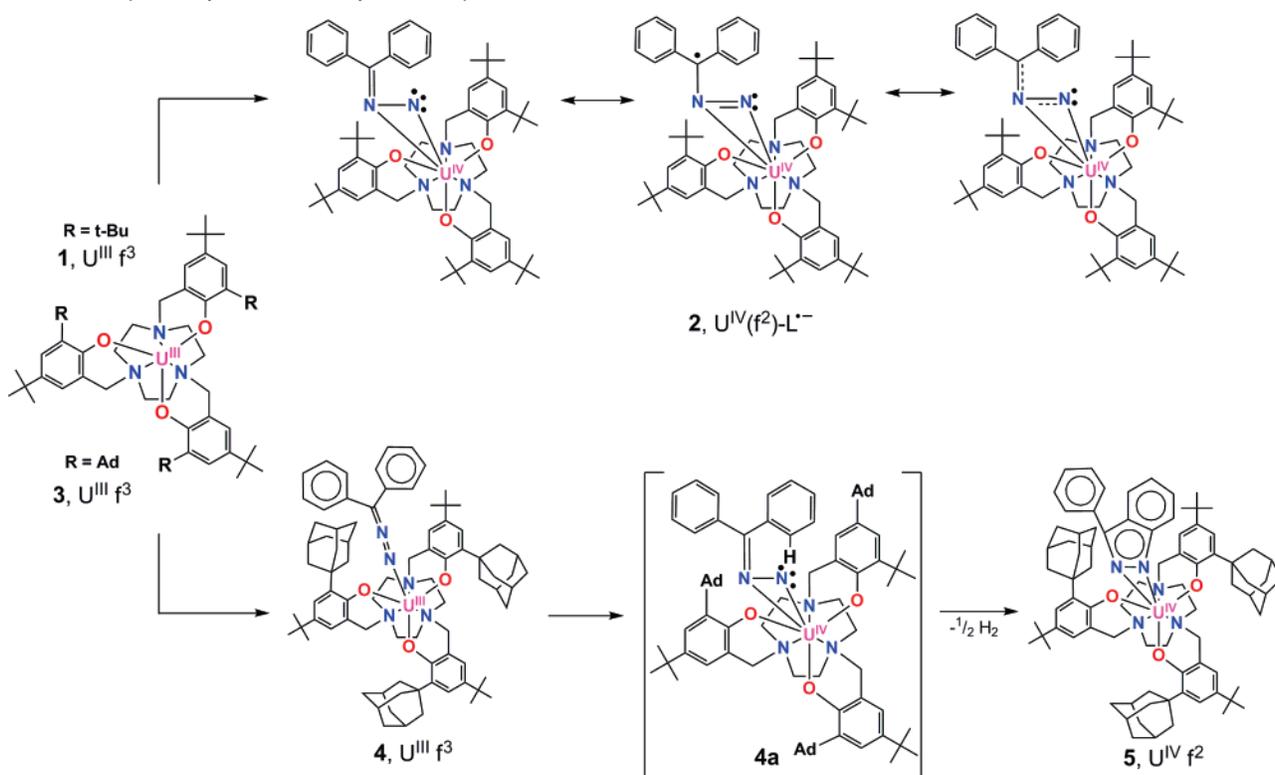
CPh$_2$))].[22] Also of interest to note is Chisholm's work featuring the formation of a diphenyldiazomethane coordinated to tungsten in an η^1 bent fashion, [W$_2$(μ-CSiMe$_3$)$_2$(CH$_2$SiMe$_3$)$_4$(N$_2$CPh$_2$)]. Heating this complex to 120 °C promotes a speculated ortho-metalation compound supported by NMR.[39] Curtis has also reported on a similar complex of a di-*p*-tolyldiazomethane complex bound in an η^1 fashion, [Cp$_2$Mo$_2$-(CO)$_3$[C(C$_6$H$_4$-*p*-Me)$_2$(N$_2$C(C$_6$H$_4$-*p*-Me)$_2$)].[40] Unfortunately, there are no reported IR stretches for the C–N–N stretch of these compounds for comparison with the proposed η^1 linear bound complex **4**.

Although complex **5** resulted from **4**, the exact mechanism of this transformation is still unknown. There is reason to assume that there must be a fleeting second intermediate **4a** between complex **4** and **5** during heating to facilitate C–H activation and nitrogen insertion to produce the indazole complex (Scheme 4). We propose this intermediate as an η^2-N,N bound complex [((^{Ad}ArO)$_3$tacn)U^{IV}(η^2-NNCPh$_2$)] that is structurally similar and electronically identical to complex **2**. Steric pressure from the adamantyl groups promotes C–H activation. This is followed by nitrogen insertion of intermediate **4a** leading to a transition state where the hydrogen resides on the nitrogen, and the U center is finally reduced back to U(III). Subsequently, hydrogen is evolved via reduction of the coordinated amine hydrogen, which has been detected by GC-TCD, and complex **5** is produced (see Experimental Section).

In the context of H$_2$ elimination from a possible intermediate on route to indazolido complex **5**, U(III) precursor **3** was treated with 1 equiv of 1H-indazole. As reported, dihydrogen elimination is commonly observed for reactions of U(III) complexes

with R–OH leading to formation of U^{IV}–OR complexes.[41–43] Presumably, reactions of U(III) complexes with R$_2$N–H would correspondingly form U^{IV}–NR$_2$ complexes. In this case, a single electron reduction of commercially available 1H-indazole produces 0.5 equiv of H$_2$ and a U(IV) complex with a mono-anionic amide-type indazolido ligand [((^{Ad}ArO)$_3$tacn)U^{IV}-(η^2-Ind)] (**6**) (Scheme 5). Green single crystals of **6** suitable for X-ray diffraction were obtained by diffusing acetonitrile into a benzene solution. Analysis of a single crystal of **6** confirms the indazolido ligand coordinated in an η^2-N,N fashion to the uranium center (Figure 9, top). With the exception of a phenyl ring in the 3-position, the coordination sphere in **6** is similar to 3-phenyl indazole complex **5**, which resulted from C–H activation and N-insertion of Ph$_2$CN$_2$. The U1–N4 and U1–N5 bond lengths of 2.381(12) Å and 2.598(8) Å in **6** are comparable to those of **5**. However, the lack of the phenyl substituent results in decreased sterics for **6**, creating linear coordination of the indazolido ligand, which bisects the three adamantyl substituents leading to an idealized C_s symmetry. Hence, the three- and five-membered rings are nearly coplanar with a dihedral angle of 2.75° (Figure 9, bottom) (as opposed to 19.2° observed in **5**).

The uranium out-of-plane shift for **6** of −0.150 Å is significantly smaller than that of complex **5** (U_{oop} = −0.265 Å). As discussed above, this U_{oop} value indicates that the U–N interaction in **6** is stronger than that in **5**. This difference in bonding interaction can also be attributed to the ability of the

(39) Chisholm, M. H.; Heppert, J. A.; Huffman, J. C.; Ontiveros, C. D. *Organometallics* **1989**, *8*, 976–982.
(40) Curtis, M. D.; Messerle, L.; D'Errico, J. J.; Butler, W. M.; Hay, M. S. *Organometallics* **1986**, *5*, 2283–2294.

(41) Clark, D. L.; Sattelberger, A. P.; Sluys, W. G. V. D.; Watkin, J. G. *J. Alloys Compd.* **1992**, *180*, 303.
(42) Wayne, W.; Lukens, J.; Beshouri, S. M.; Blosch, L. L.; Andersen, R. A. *J. Am. Chem. Soc.* **1996**, *118*, 901–902.
(43) Karmazin, L.; Mazzanti, M.; Pecaut, J. *Inorg. Chem.* **2003**, *42*, 5900–5908.

Scheme 5. Synthesis of Complex [((AdArO)₃tacn)UIV(η²-Ind)] (6)
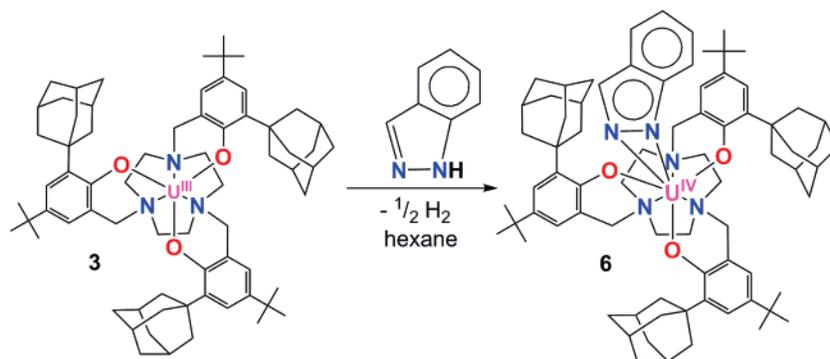
less sterically hindered indazolido ligand in **6** to more effectively penetrate the uranium core, thereby allowing for better M−L interaction.
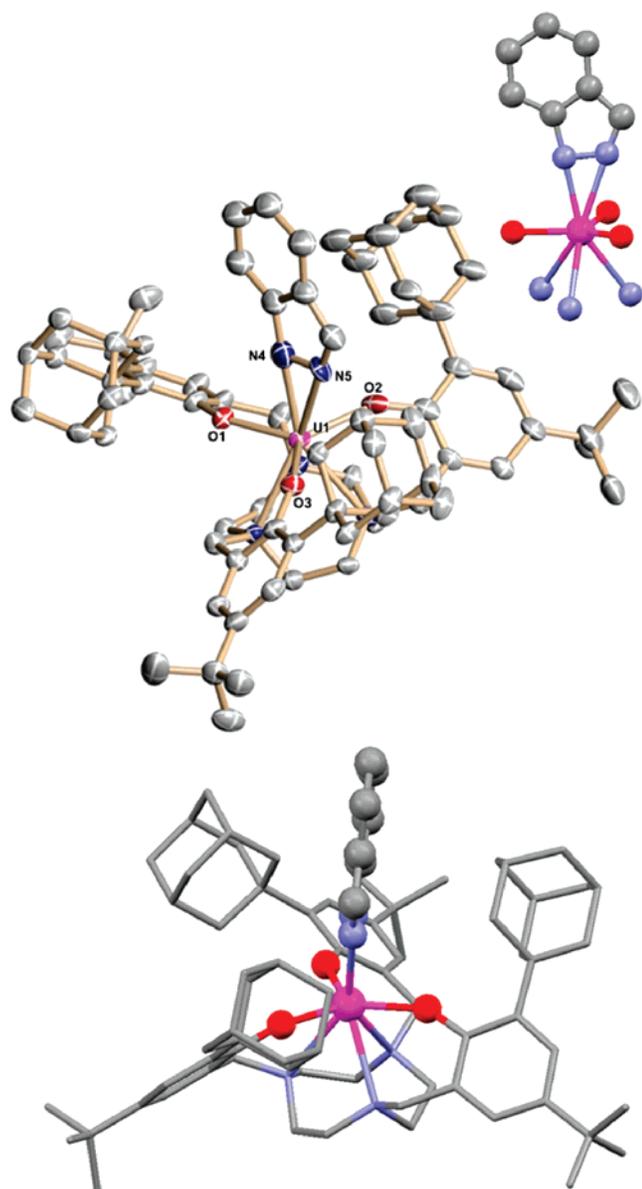

Figure 9. Molecular structure of [((AdArO)₃tacn)UIV(η²-Ind)] in crystals of **6**·C₆H₆/CH₃CN (top). Thermal ellipsoids are at the 50% probability level. Hydrogen atoms and cocrystallized solvents are omitted for clarity. Ball and stick representation of complex **6** (bottom) displays the coplanarity of the coordinated indazolido ligand.

Conclusion

The propensity of uranium complexes to act as one-electron reducing agents when combined with careful control of the molecular architecture can give rise to interesting and novel transformation chemistry, including the formation of charge-separated complexes. In the case of the η^2-diphenyldiazomethane charge-separated complex [((t^{-Bu}ArO)₃tacn)UIV(η^2-NNCPh₂)] (**2**), no further chemical transformation occurs. Increasing the steric pressure with adamantyl substituents produces the first actinide indazolido complex [((AdArO)₃tacn)UIV(η^2-3-phen-(Ind))] (**5**), presumably through the charge-separated η^2-diphenyldiazomethane intermediate, **4a**, analogous to the *tert*-butyl derivatized complex **2**. The significant impact of sterics is highlighted by use of the adamantyl ligand substituents, which create the desirable conformation for complex **4** to achieve C−H activation and nitrogen insertion. The introduction of a wider variety of ligand sterics and the exploration of the uranium complexes' reactivity is of continued interest in our group and will hopefully result in the synthesis of exciting new molecules via chemical transformation of a coordinated ligand.

Experimental Section

General Methods. All experiments were performed under a dry nitrogen atmosphere using standard Schlenk techniques or an MBraun inert-gas glovebox. Solvents were purified using a two-column solid-state purification system (Glasscontour System, Irvine, CA) and transferred to the glovebox without exposure to air. NMR solvents were obtained from Cambridge Isotope Laboratories, degassed, and stored over activated molecular sieves prior to use.

Methods. Magnetism data of crystalline powdered samples (20−30 mg) were recorded with a SQUID magnetometer (Quantum Design) at 10 kOe between 5 and 300 K for all samples. Values of the magnetic susceptibility were corrected for the underlying diamagnetic increment ($\chi_{dia} = -889.44 \times 10^{-6}$ cm³ mol⁻¹ (**2**), -1061.18×10^{-6} cm³ mol⁻¹ (**4**), -1047.25×10^{-6} cm³ mol⁻¹ (**5**)) by using tabulated Pascal constants and the effect of the blank sample holders (gelatin capsule/straw). Samples used for magnetization measurement were recrystallized multiple times and checked for chemical composition and purity by elemental analysis (C, H, and N) and ¹H NMR spectroscopy. Data reproducibility was also carefully checked on independently synthesized samples.

¹H NMR spectra (400 or 500 MHz) were recorded at a probe temperature of 20 °C on Varian (Mercury 400 or Unity 500) in C₆D₆. Chemical shifts were referenced to protio solvent impurities (δ 7.15 (C₆D₆)) and are reported in ppm.

Infrared spectra (400−4000 cm⁻¹) of solid samples were obtained on a Thermo Nicolet Avatar 360 FT-IR spectrophotometer as KBr pellets or nujol mull.

Electronic absorption spectra were recorded from 200 to 2500 nm (Shimadzu (UV-3101PC)).

Results from elemental analysis were obtained from the Analytical Laboratories at the Friedrich-Alexander-University Erlangen-Nürnberg (Erlangen, Germany) on Euro EA 3000.

GC-TCD results were obtained from the Analytical Laboratories at the Friedrich-Alexander-University Erlangen-Nürnberg (Erlangen, Germany) on a Shimadzu GC 17A, equipped with a 60 m × 0.54 mm fused silica PLOT column and thermal conductivity detector. Measurements were made with N_2 carrier gas at 70 °C.

Starting Materials. [(THF)$_4$UI$_3$] and [U(N(SiMe$_3$)$_2$)$_3$] were prepared as described by Clark et al.[44−46] Uranium turnings were purchased from Oak Ridge National Laboratory (ORNL) and activated according to literature procedures. Diphenyldiazomethane was synthesized based on literature procedures.[47] 1H-Indazole (99%) was purchased from Aldrich and used as received.

Complex Synthesis. [(($^{t-Bu}$ArO)$_3$tacn)U^{III}] (1). A solution of [U[N(SiMe$_3$)$_2$]$_3$] (1.5 g, 2.09 mmol) in hexane (17 mL) was added to a solution of 1,4,7-tris(3,5-di-*tert*-butyl-2-hydroxybenzyl)-1,4,7-triaza-cyclononane (($^{t-Bu}$ArOH)$_3$tacn) (1.55 g, 1.98 mmol) in hexane (20 mL) and stirred for 12 h at room temperature. The resulting red-brown solution was filtered and stored at −40 °C. Within 12 h, a red-brown microcrystalline precipitate formed, was filtered, washed with cold hexane, and dried under vacuum (yield: 1.39 g, 1.36 mmol, 69%). ^{1}H NMR (400 MHz, benzene-d_6, 20 °C): δ = 12.19 (s, 3H, $\Delta\nu_{1/2}$ = 15.7 Hz), 9.05 (s, 3H, $\Delta\nu_{1/2}$ = 12.7), 4.15 (s, 27H, $\Delta\nu_{1/2}$ = 15.6 Hz), 2.63 (s, 27H, $\Delta\nu_{1/2}$ = 7.08 Hz), −1.53 (s, 3H, $\Delta\nu_{1/2}$ = 41.4 Hz), −4.01 (s, 3H, $\Delta\nu_{1/2}$ = 20.8 Hz), −7.43 (s, 3H, $\Delta\nu_{1/2}$ = 23.7 Hz), −12.41 (s, 3H, $\Delta\nu_{1/2}$ = 44.1 Hz), −18.98 (s, 3H, $\Delta\nu_{1/2}$ = 32.9 Hz), −21.84 (s, 3H, $\Delta\nu_{1/2}$ = 45.1 Hz). Elemental analysis (%) calcd for **2**: C, 60.10; H, 4.12; N, 7.71. Found: C, 60.02; H, 4.18; N, 7.84.

[((^{Ad}ArO)$_3$tacn)U^{III}] (3). A solution of [U[N(SiMe$_3$)$_2$]$_3$] (0.719 g, 1.0 mmol) in benzene (10 mL) was added to a solution of 1,4,7-tris-(3-adamantyl-5-*tert*-butyl-2-hydroxybenzyl)- 1,4,7-triazacyclononane ((^{Ad}ArOH)$_3$tacn) (1.02 g, 1.0 mmol) in benzene (10 mL) and stirred for 12 h at room temperature. The resulting red-brown solution was filtered, and the volatiles were removed from filtrate under vacuum to give a red-brown solid. This was washed with pentane to obtain **3** as a red-brown solid (yield: 860 mg, 0.68 mmol, 68%). ^{1}H NMR (500 MHz, benzene-d_6, 25 °C): δ = −21.99 (s, 3H, $\Delta\nu_{1/2}$ = 16.9 Hz), −9.62 (s, 3H, $\Delta\nu_{1/2}$ = 30.6 Hz), −5.80 (s, 3H, $\Delta\nu_{1/2}$ = 13.0 Hz), −5.07 (s, 3H, $\Delta\nu_{1/2}$ = 50.3 Hz), −3.44 (s, 3H, $\Delta\nu_{1/2}$ = 4.2 Hz), −4.44 (impurity (<1H), $\Delta\nu_{1/2}$ = 18.2 Hz), −1.78 (d, 9H, $\Delta\nu_{1/2}$ = 13.9 Hz), −0.21 (d, 9H), 0.25 (d, 9H), 2.18 (s, 27H, $\Delta\nu_{1/2}$ = 45.1 Hz), 3.18 (s, 9H, $\Delta\nu_{1/2}$ = 21.3 Hz), 4.37 (s, 9H, $\Delta\nu_{1/2}$ = 29.0 Hz), 7.77 (s, 3H, $\Delta\nu_{1/2}$ = 5.7 Hz), 10.27 (s, 3H, $\Delta\nu_{1/2}$ = 5.7 Hz), 13.47 (s, 3H, $\Delta\nu_{1/2}$ = 42.8 Hz). Elemental analysis (%) calcd for **1**: C, 66.11; H, 7.72; N, 3.35. Found: C, 66.25; H, 7.68; N, 3.31.

[(($^{t-Bu}$ArO)$_3$tacn)U^{IV}(η^2-NNCPh$_2$)] (2). A pentane solution (0.5 mL) of diphenyldiazomethane (19 mg, 0.1 mmol) was added dropwise to [(($^{t-Bu}$ArO)$_3$tacn)U^{III}] (**2**) (100 mg, 0.1 mmol) in pentane (8 mL). The reaction was allowed to proceed at room temperature for 12 h. The resulting solution was filtered, concentrated, and placed in the freezer at −40 °C. Within 2 days, single orange crystals suitable for X-ray diffraction were obtained as **2**·2C$_5$H$_{12}$. The crystals can be isolated by vacuum filtration, washed with pentane, and dried to produce a fine orange powder (yield: 75 mg, 0.062 mmol, 62%). ^{1}H NMR (400 MHz, benzene-d_6, 20 °C): δ = 23.65 (s, 2H, $\Delta\nu_{1/2}$ = 25.1 Hz), 20.7 (t, 1H, $\Delta\nu_{1/2}$ = 3.17 Hz), 2.32 (t, 1H, $\Delta\nu_{1/2}$ = 2.84 Hz), 1.59 (s, 1H, $\Delta\nu_{1/2}$ = 2.35 Hz), 1.16 (m, 9H, $\Delta\nu_{1/2}$ = 18.8 Hz), 0.79 (s, 1H, $\Delta\nu_{1/2}$ = 1.31

Hz), 0.78 (d, 6H, $\Delta\nu_{1/2}$ = 1.15 Hz), −0.44 (s, 1H, $\Delta\nu_{1/2}$ = 3.52 Hz), −2.50 (s, 2H, $\Delta\nu_{1/2}$ = 2.92 Hz), −3.50 (s, 36H, $\Delta\nu_{1/2}$ = 25.2 Hz), −3.70 (s, 6H, $\Delta\nu_{1/2}$ = 13.5 Hz), −9.40 (s, 4H, $\Delta\nu_{1/2}$ = 5.12 Hz), −10.73 (s, 18H, $\Delta\nu_{1/2}$ = 334 Hz). Elemental analysis (%) calcd for **3**: C, 63.35; H, 7.31; N, 5.77. Found: C, 63.77; H, 7.13; N, 5.80.

[((^{Ad}ArO)$_3$tacn)U^{III}(η^1-NNCPh$_2$)] (4). To a solution of [((^{Ad}-ArO)$_3$tacn)U^{III}] (**1**) (250 mg, 0.2 mmol) in hexane (8 mL), diphenyl-diazomethane (39 mg, 0.2 mmol) was added. Stirring the reaction mixture for 1 h at room temperature resulted in a green-orange precipitate in an orange solution. The green-orange powder was collected by vacuum filtration and dried (yield: 200 mg, 0.14 mmol, 70%). ^{1}H NMR (400 MHz, benzene-d_6, 20 °C): δ = 23.43 (s, 3H, $\Delta\nu_{1/2}$ = 40.5 Hz), 21.93 (s, 3H, $\Delta\nu_{1/2}$ = 40.5 Hz), 13.53 (s, 1H, $\Delta\nu_{1/2}$ = 25.2 Hz), 11.74 (t, 1H, $\Delta\nu_{1/2}$ = 5.15 Hz), 10.14 (s, 1H, $\Delta\nu_{1/2}$ = 33.7 Hz), 7.82 (s, 3H, $\Delta\nu_{1/2}$ = 14.2 Hz), 6.27 (s, 3H, $\Delta\nu_{1/2}$ = 5.10 Hz), 4.09 (s, 8H, $\Delta\nu_{1/2}$ = 25.1 Hz), 3.99 (s, 2H, $\Delta\nu_{1/2}$ = 7.05 Hz), 2.66 (s, 9H, $\Delta\nu_{1/2}$ = 10.2 Hz), 2.56 (d, 9H, $\Delta\nu_{1/2}$ = 19.5 Hz), 1.84 (d, 9H, $\Delta\nu_{1/2}$ = 19.3 Hz), 1.19 (s, 6H, $\Delta\nu_{1/2}$ = 12.8 Hz), 0.84 (t, 6H, $\Delta\nu_{1/2}$ = 3.45 Hz), 0.19 (s, 27H, $\Delta\nu_{1/2}$ = 2.83 Hz), −1.02 (s, 9H, $\Delta\nu_{1/2}$ = 25.7 Hz), −3.36 (s, 1H, $\Delta\nu_{1/2}$ = 52.5 Hz), −4.21 (s, 2H, $\Delta\nu_{1/2}$ = 22.7 Hz), −32.83 (s, 3H, $\Delta\nu_{1/2}$ = 61.6 Hz). Elemental analysis (%) calcd for **4**: C, 68.03; H, 7.38; N, 4.84. Found: C, 67.89; H, 7.76; N, 4.44.

[((^{Ad}ArO)$_3$tacn)U^{IV}(η^2-3-phen(Ind))] (5). A solution of [((^{Ad}-ArO)$_3$tacn)U^{III}(η^1-NNCPh$_2$)] (**4**) (150 mg, 0.1 mmol) in benzene (10 mL) was heated at 60 °C while stirring for 2 h. The orange solution was filtered, and the volatiles were removed from the filtrate by vacuum. The yellow-green solids were washed with pentane and dried in vacuo. Recrystallization of the crude solids by slow diffusion of acetonitrile into tetrahydrofuran produced single crystals of **5** suitable for X-ray diffraction analysis (yield: 120 mg, 0.083 mmol, 83%). ^{1}H NMR (400 MHz, benzene-d_6, 20 °C): δ = 44.48 (d, 1H, $\Delta\nu_{1/2}$ = 26.2 Hz), 19.37 (s, 6H, $\Delta\nu_{1/2}$ = 172 Hz), 17.05 (s, 2H, $\Delta\nu_{1/2}$ = 115 Hz), 14.55 (s, 6H, $\Delta\nu_{1/2}$ = 233 Hz), 9.16 (s, 3H, $\Delta\nu_{1/2}$ = 118 Hz), 4.79 (s, 12H, $\Delta\nu_{1/2}$ = 19.9 Hz), 3.12 (s, 33H, $\Delta\nu_{1/2}$ = 25.6 Hz), 2.82 (s, 27H, $\Delta\nu_{1/2}$ = 21.6 Hz), 2.27 (s, 1H, $\Delta\nu_{1/2}$ = 10.4 Hz), 2.24 (t, 1H, $\Delta\nu_{1/2}$ = 3.52 Hz), 1.19 (d, 1H, $\Delta\nu_{1/2}$ = 3.83 Hz), 1.05 (t, 1H, $\Delta\nu_{1/2}$ = 4.15 Hz), 0.83 (d, 1H, $\Delta\nu_{1/2}$ = 103.6 Hz), 0.58 (d, 1H, $\Delta\nu_{1/2}$ = 4.45 Hz), −1.08 (t, 2H, $\Delta\nu_{1/2}$ = 4.15 Hz), −1.42 (t, 1H, $\Delta\nu_{1/2}$ = 3.35 Hz), −3.96 (s, 2H, $\Delta\nu_{1/2}$ = 4.25 Hz), −7.06 (s, 2H, $\Delta\nu_{1/2}$ = 117 Hz), −14.75 (s, 1H, $\Delta\nu_{1/2}$ = 13.2 Hz); −33.99 (s, 1H, $\Delta\nu_{1/2}$ = 34.8 Hz). Elemental analysis (%) calcd for **6**: C, 68.07; H, 7.32; N, 4.84. Found: C, 67.64; H, 7.48; N, 4.61.

[((^{Ad}ArO)$_3$tacn)U^{IV}(1,2-η^2-(Ind))] (6). A solution of 1H-indazole (19 mg, 0.16 mmol) in hexane (0.5 mL) was added to [((^{Ad}ArO)$_3$tacn)-U^{III}] (**6**) (200 mg, 0.16 mmol) in hexane (10 mL). The reaction mixture stirred at room temperature for 12 h. The resulting dark green precipitate in an orange solution was collected by vacuum filtration and washed with hexane. Recrystallization of the crude material by slow diffusion of acetonitrile into benzene yielded single crystals of **6**·C$_6$D$_6$/CH$_3$CN suitable for an X-ray diffraction study (yield: 90 mg, 0.066 mmol, 41%). ^{1}H NMR (270 MHz, benzene-d_6, 20 °C): δ = 12.44 (s, 1H, $\Delta\nu_{1/2}$ = 8.35 Hz), 9.31 (s, 3H, $\Delta\nu_{1/2}$ = 23.3 Hz), 7.67 (s, 3H, $\Delta\nu_{1/2}$ = 25.1 Hz), 6.35 (s, 2H, $\Delta\nu_{1/2}$ = 4.35 Hz), 5.74 (s, 2H, $\Delta\nu_{1/2}$ = 22.7 Hz), 5.28 (s, 1H, $\Delta\nu_{1/2}$ = 1.10 Hz), 4.15 (s, 2H, $\Delta\nu_{1/2}$ = 24.5 Hz), 3.25 (s, 2H, $\Delta\nu_{1/2}$ = 5.25 Hz), 2.96 (s, 3H, $\Delta\nu_{1/2}$ = 12.3 Hz), 2.56 (s, 2H, $\Delta\nu_{1/2}$ = 18.2 Hz), 2.21 (s, 2H, $\Delta\nu_{1/2}$ = 12.8 Hz), 1.86 (m, 18H, $\Delta\nu_{1/2}$ = 8.75 Hz), 1.55 (s, 9H, $\Delta\nu_{1/2}$ = 16.6 Hz), 1.26 (m, 9H, $\Delta\nu_{1/2}$ = 16.9 Hz), 1.03 (s, 3H, $\Delta\nu_{1/2}$ = 5.15 Hz), 0.85 (s, 6H, $\Delta\nu_{1/2}$ = 19.2 Hz), 0.50 (m, 4H, $\Delta\nu_{1/2}$ = 3.55 Hz), −4.21 (s, 3H, $\Delta\nu_{1/2}$ = 8.05 Hz), −4.53 (s, 6H, $\Delta\nu_{1/2}$ = 6.55 Hz), −4.63 (s, 3H, $\Delta\nu_{1/2}$ = 5.25 Hz), −5.78 (s, 3H, $\Delta\nu_{1/2}$ = 24.2 Hz), −6.09 (s, 2H, $\Delta\nu_{1/2}$ = 20.5 Hz), −7.28 (s, 2H, $\Delta\nu_{1/2}$ = 18.4 Hz), −8.48 (s, 1H, $\Delta\nu_{1/2}$ = 17.5 Hz), −9.67 (s, 3H, $\Delta\nu_{1/2}$ = 26.3 Hz), −10.94 (s, 2H, $\Delta\nu_{1/2}$ = 58.9 Hz), −11.50 (s, 1H, $\Delta\nu_{1/2}$ = 44.1 Hz), −13.10 (s, 2H, $\Delta\nu_{1/2}$ = 33.3 Hz), −15.71 (s, 1H, $\Delta\nu_{1/2}$ = 28.7 Hz).

Crystallographic Details. Crystallographic details for **2**: Orange block-shaped crystals grown from a concentrated pentane solution at

(44) Avens, L. R.; Bott, S. G.; Clark, D. L.; Sattelberger, A. P.; Watkin, J. G.; Zwick, B. D. *Inorg. Chem.* **1994**, *33*, 2248−2256.
(45) Clark, D. L.; Sattelberger, A. P.; Andersen, R. A. *Inorg. Synth.* **1997**, *31*, 307−315.
(46) Clark, D. L.; Sattelberger, A. P.; Bott, S. G.; Vrtis, R. N. *Inorg. Chem.* **1989**, *28*, 1771−1773.
(47) Miller, J. B. *J. Org. Chem.* **1959**, *24*, 560−561.

−40 °C were coated with Paratone N oil on a microscope slide. A crystal of approximate dimensions $0.10 \times 0.05 \times 0.05$ mm^3 was selected and mounted on a nylon loop. A total of 59 650 reflections ($-18 \leq h \leq 18$, $-25 \leq k \leq 24$, $-31 \leq l \leq 31$) were collected at $T = 100(2)$ K in the θ range from 2.93° to 27.10°, of which 15 355 were unique ($R_{int} = 0.0700$); Mo Kα radiation ($\lambda = 0.71\,073$ Å). The structure was solved by Direct Methods (Shelxtl Version 6.10, Bruker AXS, Inc., 2000). With the exception of hydrogen atoms, all atoms were refined anisotropically. Hydrogen atoms were placed in calculated idealized positions. The residual peak and hole electron density were 1.007 and −0.602 eA^{-3}. The absorption coefficient was 2.367 mm^{-1}. The least-squares refinement converged normally with residuals of $R_1 = 0.0704$, w$R_2 = 0.0938$, and GOF = 1.019 (all data). C$_{74}$H$_{112}$N$_5$O$_3$U, space group $P2_1/n$, monoclinic, $a = 14.5905(16)$ Å, $b = 19.570(2)$ Å, $c = 25.554(3)$ Å, $\beta = 93.452(2)°$, $V = 6998.3(14)$ Å^3, $Z = 4$, $\rho_{calcd} = 1.289$ mg/m^3, $F(000) = 2828$, $R(F) = 0.0424$, w$R(F^2) = 0.0850$ ($I > 2\sigma(I)$). CCDC reference number: 659085.

Crystallographic details for **5**: Green plate crystals grown from slow diffusion of acetonitrile into a tetrahydrofuran solution at room temperature were coated with Paratone N oil on a microscope slide. A crystal of approximate dimensions $0.30 \times 0.20 \times 0.15$ mm^3 was selected and mounted on a nylon loop. A total of 42002 reflections ($-16 \leq h \leq 15$, $-16 \leq k \leq 16$, $-31 \leq l \leq 30$) were collected at $T = 100(2)$ K in the θ range from 3.05° to 28.27°, of which 15 522 were unique ($R_{int} = 0.0271$); Mo Kα radiation ($\lambda = 0.71\,073$ Å). The structure was solved by Direct Methods (Shelxtl Version 6.10, Bruker AXS, Inc., 2000). With the exception of hydrogen atoms, all atoms were refined anisotropically. Hydrogen atoms were placed in calculated idealized positions. The residual peak and hole electron density were 1.490 and −0.731 eA^{-3}. The absorption coefficient was 2.400 mm^{-1}. The least-squares refinement converged normally with residuals of $R_1 = 0.0324$, w$R_2 = 0.0775$, and GOF = 1.049 (all data) ($I > 2\sigma(I)$). C$_{82}$H$_{105}$N$_5$O$_3$U, space group $P\bar{1}$, triclinic, $a = 12.2137(7)$ Å, $b = 12.2230(8)$ Å, $c = 23.6753(15)$ Å, $\alpha = 86.720(1)°$, $\beta = 79.248(1)°$, $\gamma = 85.654(1)°$, $V = 3459.1(4)$ Å^3, $Z = 2$, $\rho_{calcd} = 1.389$ mg/m^3, $F(000) = 1496$, $R(F) = 0.0281$, w$R(F^2) = 0.0759$ [$I > 2\sigma(I)$]. CCDC reference number: 659086.

Crystallographic details for **6**: Green block-shaped crystals grown from slow diffusion of acetonitrile into a benzene solution at room temperature were coated with Paratone N oil on a microscope slide. A crystal of approximate dimensions $0.20 \times 0.20 \times 0.15$ mm^3 was selected and mounted on a glass fiber. A total of 83 574 reflections ($-13 \leq h \leq 13$, $-21 \leq k \leq 21$, $-28 \leq l \leq 28$) were collected at $T = 100(2)$ K in the θ range from 3.05° to 27.88°, of which 17 350 were unique ($R_{int} = 0.0947$); Mo Kα radiation ($\lambda = 0.71\,073$ Å). The structure was solved by Direct Methods (Shelxtl Version 6.12, Bruker AXS, Inc., 2002). With the exception of hydrogen atoms, all atoms were refined anisotropically. Hydrogen atoms were placed in calculated idealized positions. The residual peak and hole electron density were 1.421 and −0.923 eA^{-3}. The absorption coefficient was 2.284 mm^{-1}. The least-squares refinement converged normally with residuals of $R_1 = 0.0759$, w$R_2 = 0.0888$, and GOF = 1.036 (all data). C$_{83}$H$_{110}$N$_6$O$_3$U, space group $P\bar{1}$, triclinic, $a = 10.3839(7)$ Å, $b = 16.525(2)$ Å, $c = 21.863(2)$ Å, $\alpha = 102.655(7)°$, $\beta = 91.865(8)°$, $\gamma = 95.400(6)°$, $V = 3638.7(6)$ Å^3, $Z = 2$, $\rho_{calcd} = 1.361$ mg/m^3, $F(000) = 1546$, $R(F) = 0.0440$, w$R(F^2) = 0.0798$ [$I > 2\sigma(I)$]. CCDC reference number: 659087.